Photoionization from excited Mg atoms

T. K. Fang
Institute of Atomic and Molecular Sciences, Academia Sinica, P. O. Box 23-166, Taipei, Taiwan, Republic of China 10764

T. N. Chang
Department of Physics and Astronomy, University of Southern California, Los Angeles, California 90089-0484

(Received 7 September 1999; revised manuscript received 11 January 2000; published 18 April 2000)

We present the theoretical results of a comprehensive study of the photoionization from excited Mg atoms in the spectral region below the Mg II $3p\,^2P$ limit using a *B*-spline-based configuration interaction approach. The variation of the doubly excited $^{1,3}S$, $^{1,3}P$, $^{1,3}D$, and $^{1,3}F$ resonance structures along the autoionization series is discussed. The theoretical resonant energy and width, derived from the energy variation of the scattering phase shift across each resonance, are also presented.

PACS number(s): 32.80.Fb, 32.80.Dz, 32.70.Jz, 31.25.Jf

I. INTRODUCTION

The absolute cross section of *ground-state* photoionization of a lighter alkaline-earth atom, e.g., Be and Mg, is relatively small due to the simultaneous change of electronic orbitals of two interacting outer electrons. In general, the structure profiles of the alternating broad (i.e., $np\nu s$) and narrow (i.e., $np\nu d$) ^1P resonances are fairly regular along the doubly excited autoionization series [1,2]. In contrast, the spectra from the *bound-excited* states are usually dominated by the *isolated core excitation* [3,4], i.e., a one-electron $\Delta\nu=0$ *shakeup* process of the outer excited electron following the excitation of the inner ns core electron. The resonance structures could vary substantially as ν increases. A change in the sign of the Fano q parameters [5] along the doubly excited $sp,2n^+\,^1P$ series in the He $1s2s\,^1S\rightarrow{}^1P$ photoionization has been suggested recently [6]. Photoionization from a bound-excited state also allows the possibility to study resonances with symmetries other than ^1P, which are not accessible in a one-photon process from the ground state [7].

In this paper, we present the quantitative results of a comprehensive study of the photoionization from the bound-excited $3snl\,^{1,3}S$, $^{1,3}P$, and $^{1,3}D$ states of Mg. The theoretical data are calculated using a *B*-spline-based configuration interaction (BSCI) approach [8,9]. In addition to its successful applications to the ground-state photoionization of He and alkaline-earth atoms [4,8,10], more recently, the near-threshold BSCI absolute photoionization cross sections from the bound excited $1snp\,^1P$ states of He have also been confirmed experimentally [11].

Most of the results presented in this paper are calculated using a set of basis functions which consists of all possible products of one-electron frozen core Hartree-Fock (FCHF) functions [9], including both positive and negative energy orbitals, i.e., similar to an extended CC-CC calculation detailed in [12]. The typical size of the extended BSCI basis ranges up to 9000. The Hamiltonian matrix is diagonalized using a two-step procedure discussed in [9]. The worst disagreement between length and velocity results is about 5%. In general, length-velocity agreement is substantially better than 5%. Only length results are presented in this paper. The BSCI results are also consistent with other earlier available theoretical [2,13,14] and experimental [1,7] data.

II. RESULTS AND DISCUSSIONS

The theoretical resonant energy and width of a doubly exited state are determined in the BSCI procedure [8,9] from

TABLE I. The calculated widths Γ (in $a[\mu]=a\times10^{\mu}$ Ry) and effective quantum numbers ν for the Mg $3pnp\,^{1,3}S$, the $3pns$ and $3pnd\,^{1,3}P$, the $3pnp$ and $3pnf\,^{1,3}D$, and the $3pnd$ and $3png\,^{1,3}F$ resonances converging to $3p$ limit. The energy difference between $3p$ and $3s$ limits, i.e., $\epsilon_{3p}-\epsilon_{3s}$, is 0.325 606 Ry.

Singlet			Triplet		
state	ν	Γ	state	ν	Γ
$3p^2\,^1S$	1.9550	2.88[−3]	$3p4p\,^3S$	2.8473	1.83[−6]
$3p4p\,^1S$	3.1324	5.99[−5]	$3p5p\,^3S$	3.8748	3.44[−6]
$3p5p\,^1S$	4.1442	4.62[−6]	$3p6p\,^3S$	4.8858	2.66[−6]
$3p6p\,^1S$	5.1477	7.29[−8]	$3p4s\,^3P$	2.3172	5.66[−4]
$3p4s\,^1P$	2.3967	2.79[−2]	$3p5s\,^3P$	3.3467	2.85[−4]
$3p5s\,^1P$	3.4290	8.01[−3]	$3p6s\,^3P$	4.3584	1.56[−4]
$3p6s\,^1P$	4.4401	3.45[−3]	$3p3d\,^3P$	2.8673	1.13[−3]
$3p3d\,^1P$	3.0993	1.59[−4]	$3p4d\,^3P$	3.8485	3.49[−4]
$3p4d\,^1P$	4.0908	5.54[−5]	$3p5d\,^3P$	4.8448	1.48[−4]
$3p5d\,^1P$	5.0867	2.48[−5]	$3p4p\,^3D$	2.7124	2.04[−3]
$3p4p\,^1D$	2.9395	1.95[−2]	$3p5p\,^3D$	3.7487	8.78[−4]
$3p5p\,^1D$	3.9626	1.01[−2]	$3p6p\,^3D$	4.7635	4.48[−4]
$3p6p\,^1D$	4.9474	5.21[−3]	$3p4f\,^3D$	4.0277	3.98[−5]
$3p4f\,^1D$	4.0253	2.87[−6]	$3p5f\,^3D$	5.0267	3.28[−5]
$3p5f\,^1D$	5.0225	4.92[−6]	$3p3d\,^3F$	2.5268	2.13[−2]
$3p3d\,^1F$	3.1012	6.63[−3]	$3p4d\,^3F$	3.6160	3.36[−3]
$3p4d\,^1F$	4.1165	3.63[−3]	$3p5d\,^3F$	4.6379	1.39[−3]
$3p5d\,^1F$	5.1196	2.10[−3]	$3p6d\,^3F$	5.6496	7.31[−4]
$3p6d\,^1F$	6.1251	1.27[−3]	$3p7d\,^3F$	6.6590	4.33[−4]
$3p7d\,^1F$	7.1302	8.32[−4]	$3p5g\,^3F$	5.0294	5.83[−8]
$3p5g\,^1F$	5.0294	7.57[−8]	$3p6g\,^3F$	6.0333	6.26[−8]
$3p6g\,^1F$	6.0333	9.67[−8]	$3p7g\,^3F$	7.0388	5.11[−8]
$3p7g\,^1F$	7.0388	9.35[−8]			

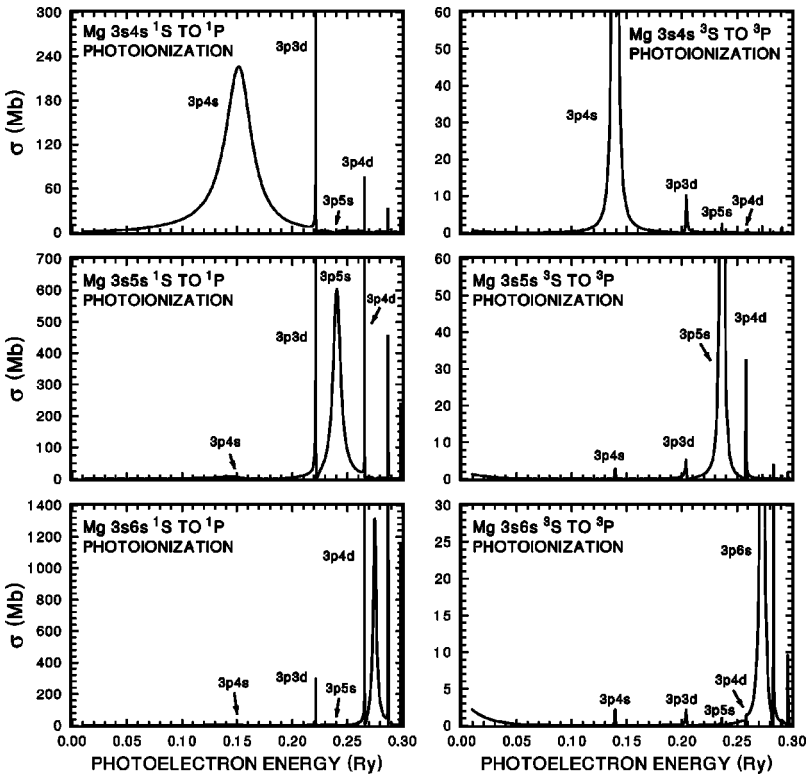

FIG. 1. Mg $^{1,3}S \rightarrow {}^{1,3}P$ photoionization from bound excited $3s\nu_i s\ {}^{1,3}S$ states.

the energy variation of the scattering phase shifts across each resonance. (We should note that the energy and width of a resonance can also be determined by a spline-Galerkin method developed by Brage *et al.* [15].) Table I summarizes the calculated widths Γ and the effective quantum number ν of the Mg $3p\nu l\ {}^{1,3}S$, $^{1,3}P$, $^{1,3}D$, and $^{1,3}F$ autoionization series converging to the Mg II $3p\ {}^2P$ limit. Except for the ^1P series, the relative energies of all autoionization series follow the usual Hund's rule, i.e., the triplet states lie below that of the singlet states in energy and the states with smaller total orbital angular momentum L lie above that of the states with larger L. Our calculation has shown that the $3p\nu d\ {}^1F$ state is located slightly above its corresponding $3p\nu d\ {}^1P$ state. This can be attributed to the stronger mixing between the doubly excited $3pd$ series and the singly excited $3sf$ series for the ^1F symmetry than that between the $3pd$ and $3sp$ series for the ^1P symmetry. This stronger configuration mixing is also responsible for the greater widths of the $3p\nu d\ {}^1F$ series than that of the $3p\nu d\ {}^1P$ series. In addition, the calculated energies of the $^{1,3}S$, $^{1,3}P$, and $^{1,3}D$ bound excited states relative to the Mg II $3p\ {}^2P$ threshold are also listed in Table II.

TABLE II. The calculated energy E (in Ry) for the Mg bound excited $3sns\ {}^{1,3}S$, $3snp\ {}^{1,3}P$, and $3snd\ {}^{1,3}D$ states relative to the Mg II $3p\ {}^2P$ limit.

Singlet		Triplet	
state	E	state	E
$3s^2\ {}^1S$	−1.66971	$3s4s\ {}^3S$	−1.29202
$3s4s\ {}^1S$	−1.27109	$3s5s\ {}^3S$	−1.19448
$3s5s\ {}^1S$	−1.18827	$3s6s\ {}^3S$	−1.15779
$3s6s\ {}^1S$	−1.15511	$3s3p\ {}^3P$	−1.47206
$3s3p\ {}^1P$	−1.34635	$3s4p\ {}^3P$	−1.23163
$3s4p\ {}^1P$	−1.21704	$3s5p\ {}^3P$	−1.17290
$3s5p\ {}^1P$	−1.16843	$3s6p\ {}^3P$	−1.14758
$3s6p\ {}^1P$	−1.14564	$3s3d\ {}^3D$	−1.23040
$3s3d\ {}^1D$	−1.24634	$3s4d\ {}^3D$	−1.17335
$3s4d\ {}^1D$	−1.18374	$3s5d\ {}^3D$	−1.14800
$3s5d\ {}^1D$	−1.15432	$3s6d\ {}^3D$	−1.13455
$3s6d\ {}^1D$	−1.13851		

A. Transitions between *S* and *P* states

Figure 1 shows that the Mg $^{1,3}S \rightarrow {}^{1,3}P$ photoionization spectra from bound excited $3s\nu_i s\ {}^{1,3}S$ states are dominated

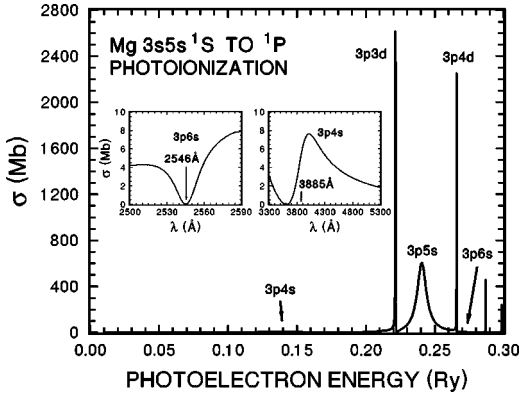

FIG. 2. Mg $3s5s\ {}^1S \rightarrow {}^1P$ photoionization. The cross section near the $3p4s\ {}^1P$ resonance on the longer wavelength side (i.e., lower energy side) is greater than the one near the $3p6s\ {}^1P$ resonance on the shorter wavelength side.

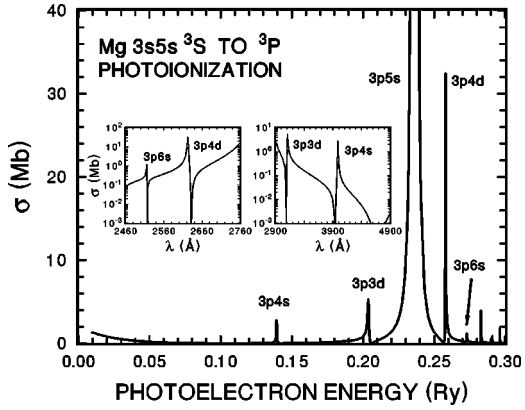

FIG. 3. The sign change of the q values of the ^3P resonances along the autoionization series in Mg $3s5s\,^3S \rightarrow {}^3P$ photoionization.

by the *shakeup* of the outer $\nu_i s$ electron following the $3s \rightarrow 3p$ core excitation. For the $3s\nu s\,^{1,3}S \rightarrow 3p(\nu \pm 1)s\,^{1,3}P$ (i.e., $\Delta\nu \neq 0$) transitions, Fig. 2 shows that the cross section on the lower-energy side is greater than that on the higher-energy side. This feature is similar to the $3s\nu d\,^1D \rightarrow 3p(\nu \pm 1)d\,^1F$ and $3s\nu p\,^1P \rightarrow 3p(\nu \pm 1)p\,^1D$ photoionization (see, e.g., Figs. 3 and 9 in [4]) due to a change in the interference pattern from *constructive* to *destructive* across the dominant $\Delta\nu = 0$ transition. Figure 3 shows that the q values of the ^3P resonances on the lower-energy side change from negative to positive along the autoionization series as the energy increases to the higher-energy side across the dominant $3s5s\,^3S \rightarrow 3p5s\,^3P$ peak. A breakdown of individual contributions to the total transition amplitudes F_t^{fi} for the photoionization from the$3s5s\,^3S$ state near the $3p4s\,^3P$ and $3p6s\ ^3P$ resonances detailed in Fig. 4 shows that F_t^{fi} is dominated by the $3ss \rightarrow 3ps$ shakeup process. As the energy increases from the $3p4s\,^3P$ resonance to the $3p6s\,^3P$ resonance, the net effect due to contributions from other processes is to change the relative positions between the zero in F_t^{fi} and the minimum of the square of the amplitude A of the oscillating radial function that represents the outgoing ionized electron. A similar feature has also been reported recently in the He $1s2s\,^1S \rightarrow sp, 2n^+\,^1P$ photoionization along the $2n^+$ autoionization series [6].

Although there are no experimental $^{1,3}S \rightarrow {}^{1,3}P$ photoionization data from the excited states that can be compared directly to the theoretical BSCI results presented in Fig. 1, the theoretical spectrum from the ground state compares very well with the observed data. In addition to the excellent theory-experiment agreement shown in Ref. [10] for the first few doubly excited resonances above the first ionization threshold, Fig. 5 shows a good agreement between the BSCI result and a recent absolute cross-section measurement at higher energy [16]. As the theoretical peak cross section of the $3p5s\,^1P$ resonance is slightly higher than the measured value, the discrepancy between theory and experiment is somewhat larger on the higher-energy shoulder near 112.5 nm.

Except for the $3p^2\,^1S$ state, the widths of all $3p\nu p\,^{1,3}S$ states are relatively small (i.e., 0.1–1 meV or less). As a result, the resonance profiles of the $3s\nu_i p\,^{1,3}P \rightarrow 3p\nu p\,^{1,3}S$ photoionization spectra are very difficult to resolve in detail as shown in Fig. 6. A closer look at the more detailed spectra

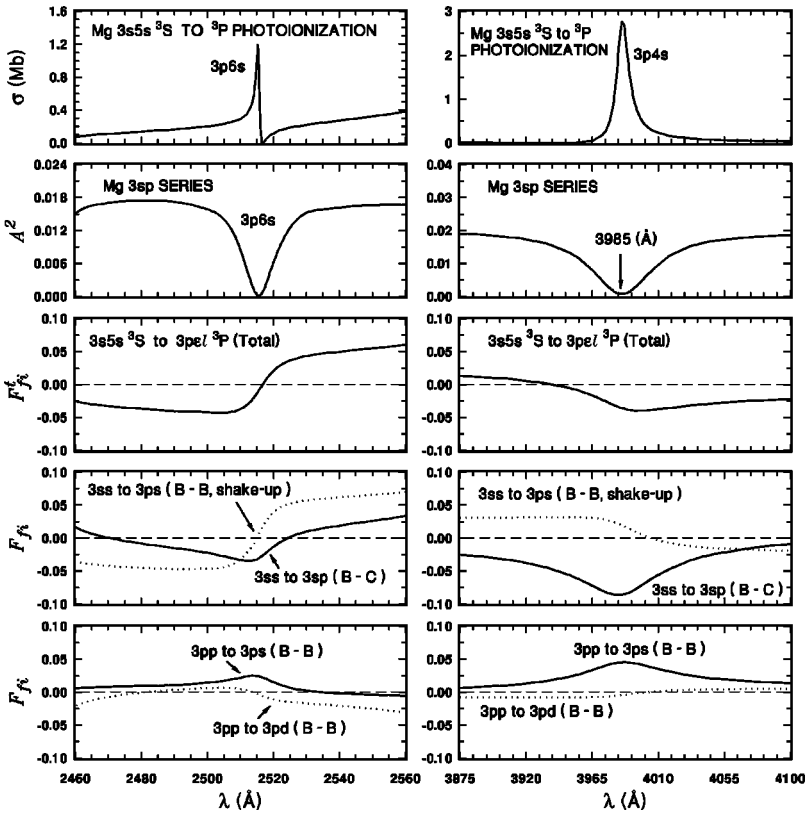

FIG. 4. Breakdown of individual contributions to the total transition amplitudes F_{fi}^t for the photoionization from $3s5s\,^3S$ state near the $3p4s\,^3P$ and $3p6s\,^3P$ resonances. See Table I and Figs. 5 and 7 of [4] for the detailed processes corresponding to the bound-to-bound (B-B) and bound-to-continuum (B-C) transitions.

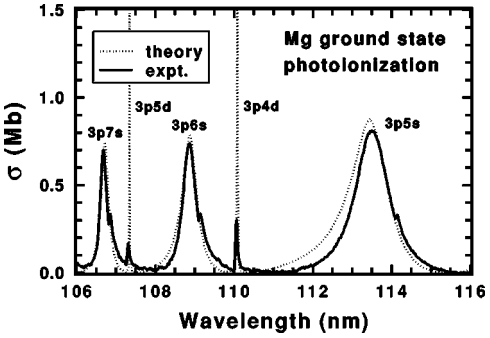

FIG. 5. Comparison between theoretical BSCI ground state Mg photoionization cross sections and the most recent photoabsorption spectrum by Yih [16].

of a number of selected resonances given in Fig. 7 shows that the $^{1,3}P \rightarrow {}^{1,3}S$ photoionization is also dominated by the $\Delta\nu=0$ *shakeup* of the outer p electron following the $3s \rightarrow 3p$ core excitation.

B. Transitions between *P* and *D* states

Figure 8 shows that the Mg $3s\nu_i p\ {}^{1,3}P \rightarrow 3p\nu l\ {}^{1,3}D$ photoionizations are similarly dominated by the *shakeup* of the outer $\nu_i p$ electron following the $3s \rightarrow 3p$ core excitation. One of the most interesting features in the $^1P \rightarrow {}^1D$ photoionization spectra is the presence of a very broad resonance located across the first ionization threshold. This broad resonance corresponds to a $3p^2\ {}^1D$ state *diluted* in a $3sd\ {}^1D$ series [14]. Figure 9 shows clearly that the probability density $\rho_{\xi_{np}}$ for the $3pnp\ {}^1D$ state, estimated from the weighted radial function ξ_{np} [defined by Eq. (10) of Ref. [8] or Eq. (50) of Ref. [9]] based on our BSCI calculation, is relatively small and varies smoothly as energy decreases. For Mg, any atomic transition which involves a ^1D state (i.e., either a bound excited $3s\nu_i d\ {}^1D$ state or a resonant $3p\nu' p\ {}^1D$ state in the continuum) is affected strongly by the strong configuration mixing between the $3sd$ and $3pp$ series [17,18]. The lack of a localized resonance feature is just one such example.

Experimentally, the $3p\nu(\geqslant 4)p\ {}^1D$ resonances were not observed in the two-photon ionization spectra from the Mg ^1S ground state in spite of a definitive identification of the overlapping doubly excited $3p\nu p\ {}^1S$ and $3p\nu f\ {}^1D$ autoionization series [19]. The *absence* of the $3p\nu p\ {}^1D$ series in the observed $^1S \rightarrow {}^1D$ two-photon ionization spectrum is consistent with the result of an earlier theoretical estimation (see, e.g., Fig. 1 in Ref. [10]). In fact, based on our calculated $3s3p\ {}^1P \rightarrow 3p\nu l\ {}^1D$ spectrum shown in Fig. 8, we may conclude that the near zero transition rate near the $3p\nu p\ {}^1D$ *window* resonances is responsible for the absence of the $3p\nu p\ {}^1D$ series in the two-photon ionization spectra.

Another example which manifests the strong $3sd-3pp$ configuration interaction can be found in the $3s\nu_i d\ {}^1D \rightarrow 3p\nu l\ {}^1P$ photoionization spectra shown in Fig. 10. Unlike the $3s\nu_i d\ {}^3D \rightarrow 3p\nu d\ {}^3P$ photoionization, which is clearly dominated only by the $\Delta\nu=0$ *shakeup* process of the outer d electron following the $3s \rightarrow 3p$ core excitation, the $3s\nu_i d\ {}^1D \rightarrow 3p\nu d\ {}^1P$ spectra are dominated by both the $3s\nu_i d\ {}^1D \rightarrow 3p\nu_i d\ {}^1P$ (i.e., $\Delta\nu=0$) *shakeup* process and the $3s\nu_i d\ {}^1D \rightarrow 3s(\nu_i-1)d\ {}^1P$ (i.e., $\Delta\nu=-1$) *shakedown* process. The large transition amplitudes for the $\Delta\nu=0$ and -1 transitions result directly from a substantial overlap between the initial $\nu_i d$ and the final $\nu' d$ orbitals, which can be

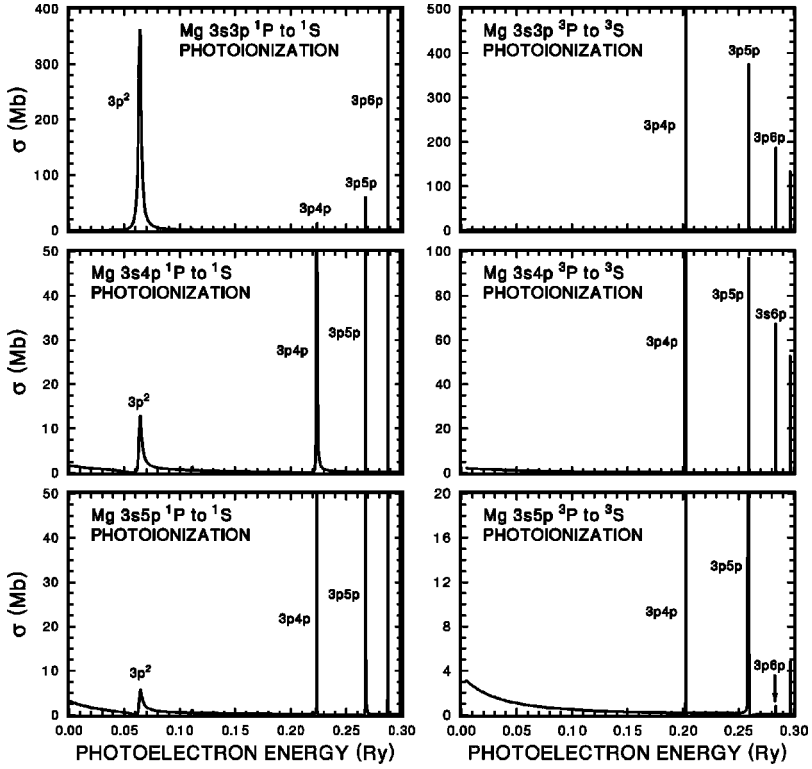

FIG. 6. Mg $^{1,3}P \rightarrow {}^{1,3}S$ photoionization from bound excited $3s\nu_i p\ {}^{1,3}P$ states.

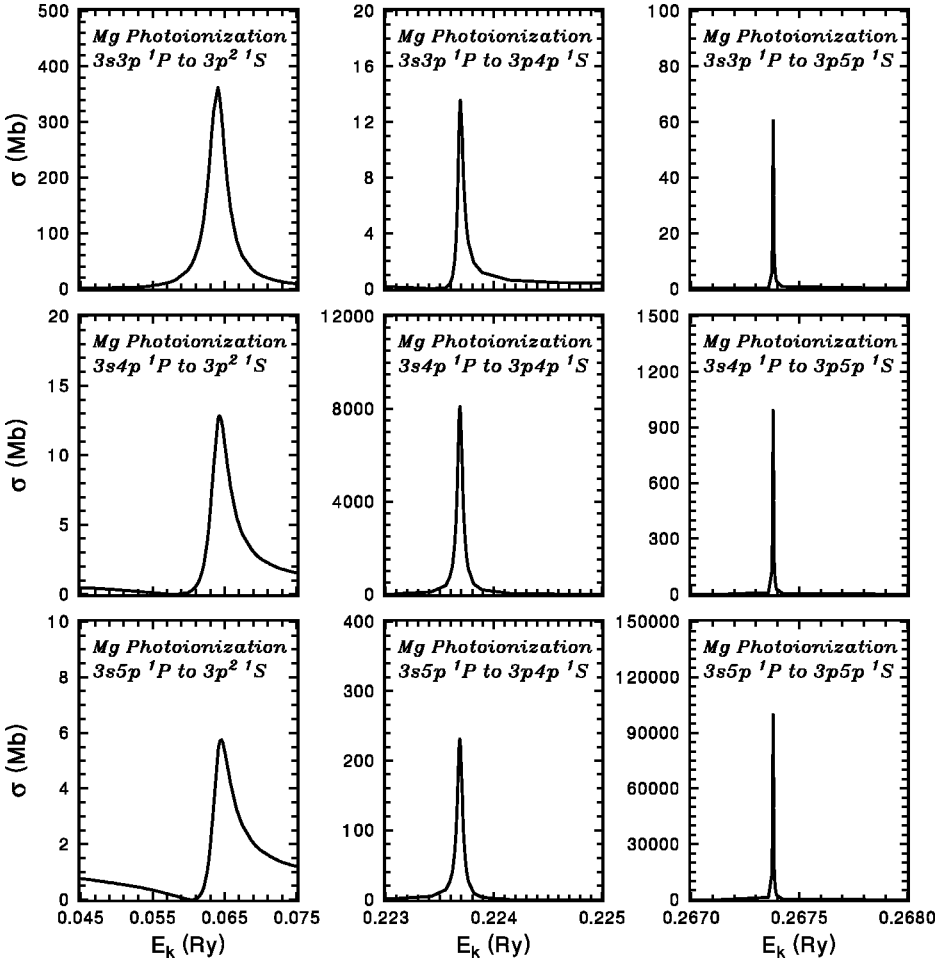

FIG. 7. Mg $^{1,3}P \rightarrow {}^{1,3}S$ photoionization spectra near $3pnp\ ^1S$ resonances from selected bound excited $3s\nu_i p\ ^{1,3}P$ states.

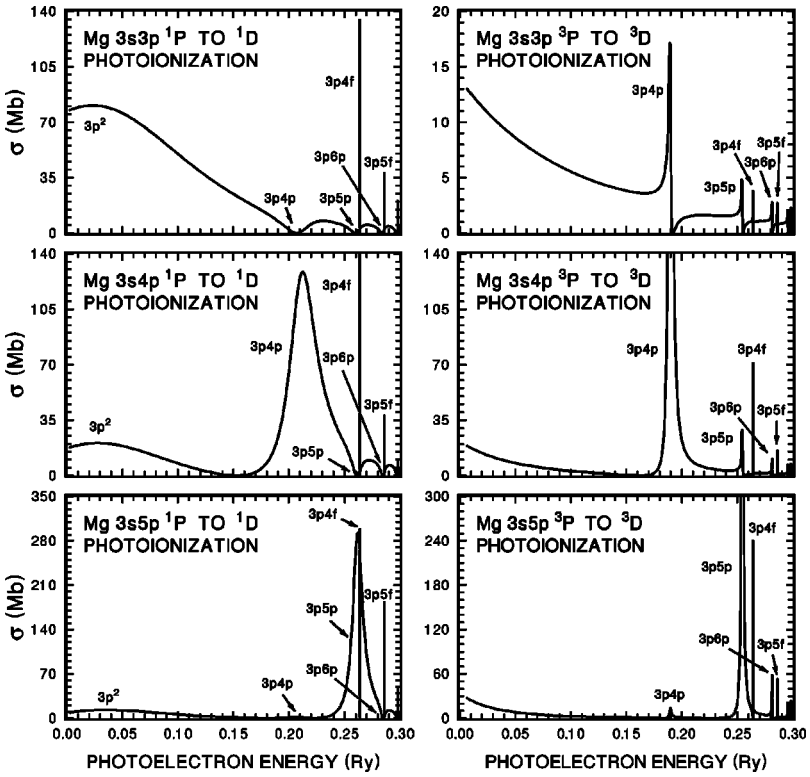

FIG. 8. Mg $^{1,3}P \rightarrow {}^{1,3}D$ photoionization from bound excited $3s\nu_i p\ ^{1,3}P$ states.

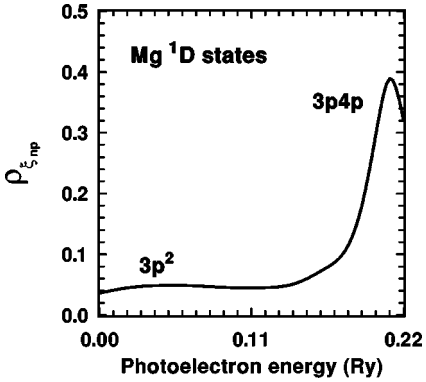

FIG. 9. The probability density $\rho_{\xi_{np}}$ for the $3pnp\,^1D$ state.

attributed, in turn, to a large negative quantum defect of the d orbitals of the $3s\nu_i d\,^1D$ series. Our BSCI calculation has shown that the respective effective principal quantum numbers of 2.66, 3.57, and 4.51 for the $3s3d$, $3s4d$, and $3s5d\,^1D$ initial states differ from the effective principal quantum numbers of 3.10, 4.09, and 5.09 for the $3p3d$, $3p4d$, and $3p5d\,^1P$ final states only by about 0.5, instead of a value close to 1.0. As a result, the rates of the $\Delta\nu=0$ and $\Delta\nu=-1$ transitions are comparable as shown. In addition, a small mixture of the $3p\nu' d$ component in the $3p\nu' s\,^1P$ state is responsible for the strong $3s\nu_i d\,^1D\rightarrow 3p(\nu_i-1)s\,^1P$ transition due to the proximity of the effective principal quantum numbers of the $3p4s$, $3p5s$, and $3p6s$ ^1P states (i.e., 2.40, 3.43, and 4.44, respectively) and that of the initial $3s\nu_i d\,^1D$ states.

Figure 11 shows that the q parameters of the resonances located on the lower-energy side of the dominating

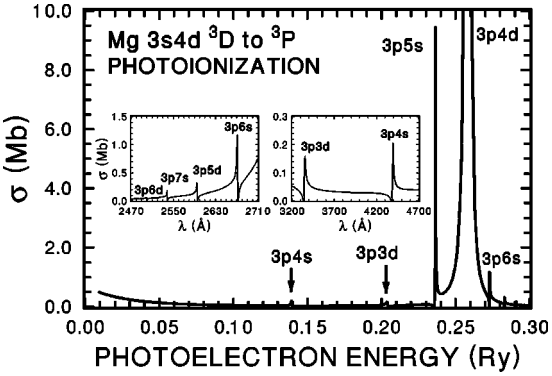

FIG. 11. The sign change of the q values of the ^3P resonances along the autoionization series in Mg $3s4d\,^3D\rightarrow{}^3P$ photoionization.

$3s4d\,^3D\rightarrow 3p4d\,^3P$ (i.e., $\Delta\nu=0$) *shakeup* peak are opposite in sign to the ones on the higher-energy side. A detailed breakdown of individual contributions to the total transition amplitudes F_t^{fi} is shown in Fig. 12. Again, this sign change of the q parameters can be accounted for by a similar physical interpretation for the $3s5s\,^3S\rightarrow{}^3P$ photoionization discussed earlier (see, e.g., Figs. 3 and 4).

C. $^{1,3}D$ to $^{1,3}F$ transitions

Our theoretical BSCI $3s\nu_i d\,^{1,3}D\rightarrow 3p\nu l\,^{1,3}F$ spectra are summarized in Fig. 13. For the $^3D\rightarrow{}^3F$ photoionization, again, the transitions are dominated by the $\Delta\nu=0$ shakeup of the outer d electron following the $3s\rightarrow 3p$ core excitation. In contrast, for the $^1D\rightarrow{}^1F$ photoionization, the $3s\nu_i d\,^1D\rightarrow 3p(\nu_i-1)d\,^1F$ (i.e., $\Delta\nu=-1$) *shakedown* process is, in

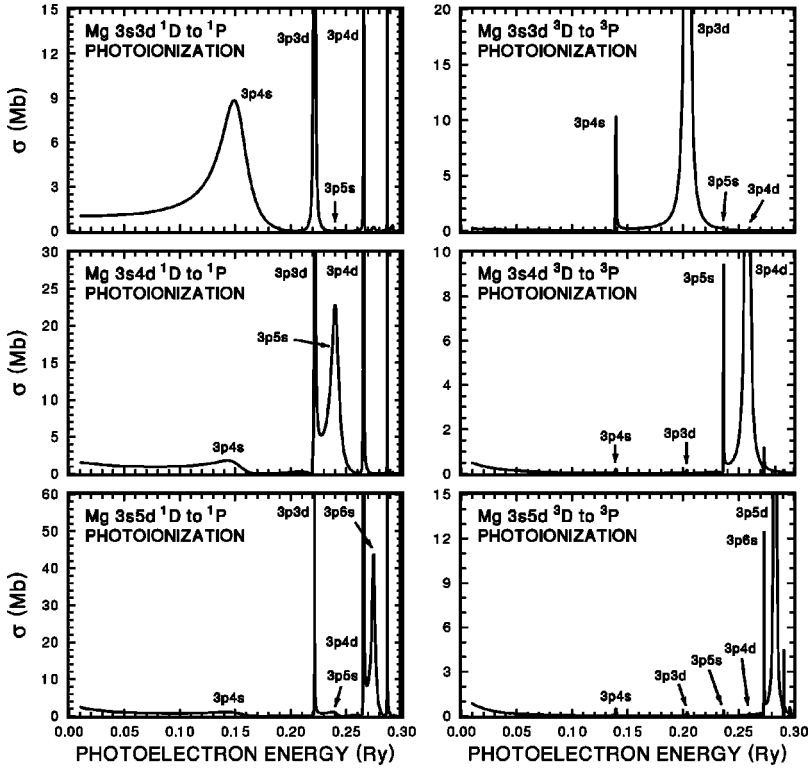

FIG. 10. Mg $^{1,3}D\rightarrow{}^{1,3}P$ photoionization from bound excited $3s\nu_i d\,^{1,3}D$ states.

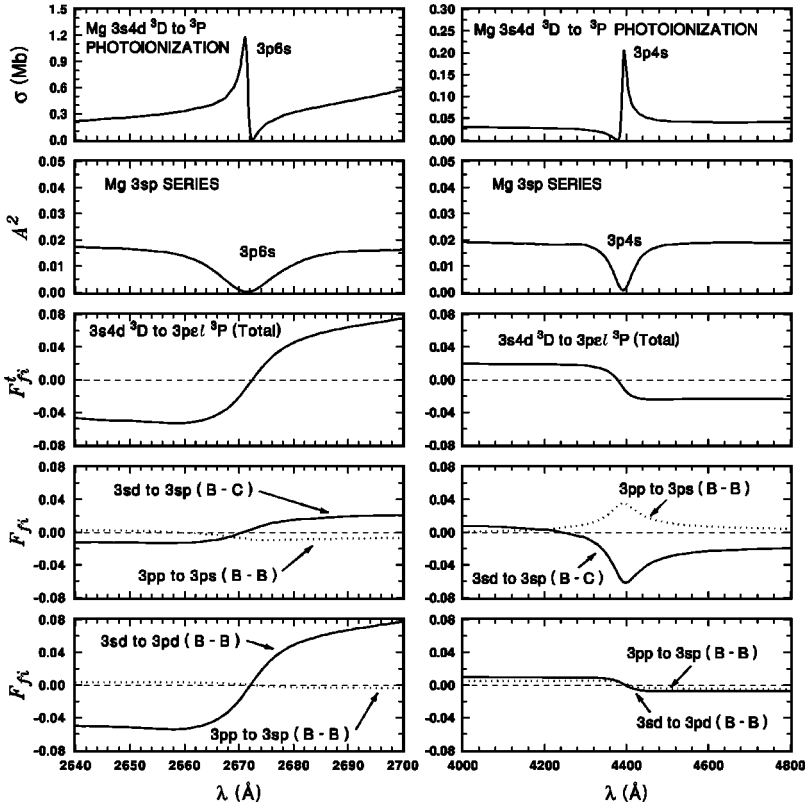

FIG. 12. Breakdown of individual contributions to the total transition amplitudes F_{fi}^{t} for the photoionization from $3s4d\,^3D$ state near the $3p4s\,^3P$ and $3p6s\,^3P$ resonances. See also Figs. 5 and 7 of [4] for the detailed processes corresponding to the bound-to-bound (B-B) and bound-to-continuum (B-C) transitions.

fact, more prominent than the $3s\nu_i d\,^1D \rightarrow 3p\nu_i d\,^1F$ (i.e., $\Delta\nu=0$) *shakeup* process. Similar to the $^1D \rightarrow {}^1P$ spectra discussed earlier, this can be attributed again to the strong $3sd-3pp$ mixing, which leads directly to a substantial overlap in effective principal quantum numbers between the $3p3d$, $3p4d$, and $3p5d\,^1F$ final states (i.e., 3.10, 4.12, and 5.12, respectively) and the $3s3d$, $3s4d$, and $3s5d\,^1D$ initial states (i.e., 2.66, 3.57, and 4.51, respectively).

For the Mg $3p\nu d\,^1F$ resonances, our BSCI calculation has confirmed what we reported recently [4] that the outer

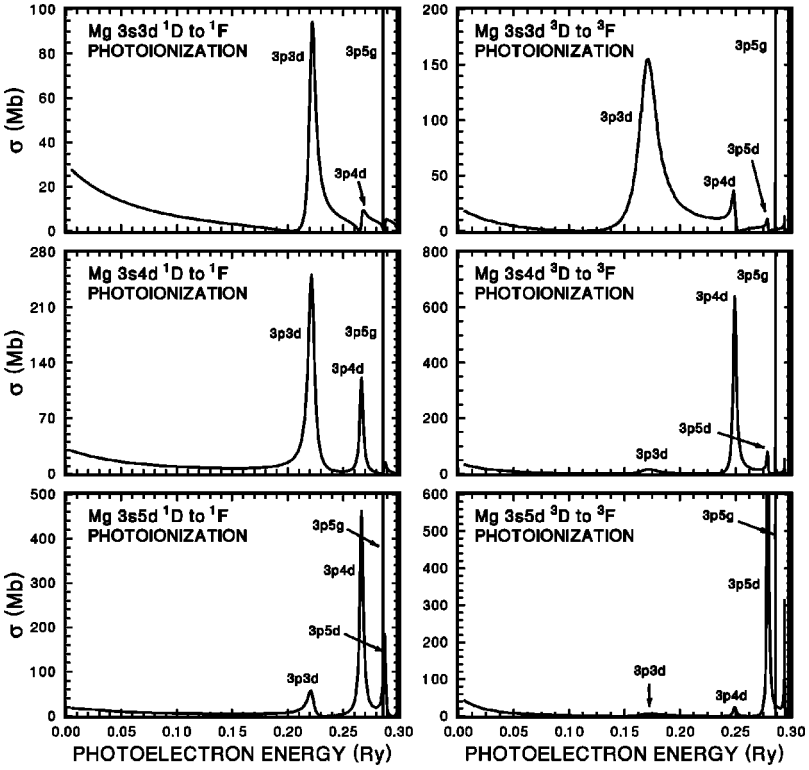

FIG. 13. Mg $^{1,3}D \rightarrow {}^{1,3}F$ photoionization from bound excited $3s\nu_i d\ {}^{1,3}D$ states.

νd electron (which is subject to slightly more screening by the inner $3s$ electron due to a substantial configuration mixing between the $3p\nu d$ and the background $3s\varepsilon f$ channel) does not penetrate as much to the small r region as the outer νg electron of the $3p\nu g\,{}^1F$ resonance. As a result, the $3p\nu d\,{}^1F$ resonance is located at the higher-energy side of the $3p\nu g\,{}^1F$ resonance. A more detailed discussion of the interference between the overlapping $3p\nu d$ and $3p\nu g\,{}^1F$ autoionization series has already been presented in Ref. [4]. Finally, we note that the very narrow $3p\nu g\,{}^1F$ series, with a resonance width of the order of a few hundred MHz, has been observed recently in a three-color stepwise laser excitation and time-of-flight mass spectrometry experiment [20].

D. Concluding remarks

In summary, the photoionization spectra from bound excited Mg in $3s\nu_i\ell\,{}^{1,3}L$ states are generally dominated by the $\Delta\nu=0$ *shakeup* process of the outer $\nu_i\ell$ electron following the one-electron $3s\rightarrow 3p$ core excitation. The only exception is when the transition is substantially affected by the strong $3sd-3pp$ mixing shown in Fig. 13. Based on a more comprehensive quantitative study on the variation of the resonance profiles along the doubly excited autoionization series presented in this paper, we are able to confirm two interesting new features which we first suggested in Refs. [4] and [6] for limited transitions only. First, in addition to the ${}^1D\rightarrow{}^1F$ transition reported in Ref. [4], the present calculation has shown that the cross section on the lower-energy side is greater than that on the higher-energy side of the dominant $\Delta\nu=0$ peak, due to a change in the interference pattern from *constructive* to *destructive*, for transitions involving all other symmetries. Second, similar to what we reported in Ref. [6] for He, a sign change in the Fano q parameter along the autoionization series in Mg has also been identified (see, e.g., Figs. 3 and 11). The detailed quantitative estimates presented in this study should further facilitate experimental observations such as the one reported recently in Ref. [20].

ACKNOWLEDGMENTS

This work was supported by NSF Grant No. PHY9802557 and the Institute of Atomic and Molecular Sciences, Academia Sinica, Taiwan, ROC.

[1] J. M. Esteva, G. Mehlman-Balloffet, and J. Romand, J. Quant. Spectrosc. Radiat. Transf. **12**, 1291 (1972); G. Mehlman-Balloffet and J. M. Esteva, Astrophys. J. **157**, 945 (1969); J. P. Preses, C. E. Burkhardt, W. P. Garver, and J. J. Leventhal, Phys. Rev. A **29**, 985 (1984); W. Fiedler, Ch. Kortenkamp, and P. Zimmermann, *ibid.* **36**, 384 (1987); T. S. Yih, H. H. Wu, H. T. Chan, C. C. Chu, and B. J. Pong, Chin. J. Phys. (Taipei) **27**, 136 (1989).

[2] G. N. Bates and P. L. Altick, J. Phys. B **6**, 653 (1973); C. Froese Fischer and H. P. Saha, Can. J. Phys. **65**, 772 (1987); R. Moccia and P. Spizzo, J. Phys. B **21**, 1145 (1988); R. Moccia and P. Spizzo, Phys. Rev. A **39**, 3855 (1989).

[3] T. A. Carlson and M. O. Krause, Phys. Rev. **140**, A1057 (1965); T. A. Carlson, Phys. Rev. **156**, 142 (1967); W. E. Cooke, T. F. Gallagher, S. A. Edelstein, and R. M. Hill, Phys. Rev. Lett. **40**, 178 (1978); R. M. Jopson, R. R. Freeman, W. E. Cooke, and J. Bokor, *ibid.* **51**, 1640 (1983); K. Butler, C. Mendoza, and C. J. Zeippen, J. Phys. B **26**, 4409 (1993).

[4] T. K. Fang, B. I. Nam, Y. S. Kim, and T. N. Chang, Phys. Rev. A **55**, 433 (1997).

[5] U. Fano, Phys. Rev. **124**, 1866 (1961).

[6] T. K. Fang and T. N. Chang, Phys. Rev. A **56**, 1650 (1997).

[7] R. E. Bonanno, C. W. Clark, and T. B. Lucatorto, Phys. Rev. A **34**, 2082 (1986); D. J. Bradley, C. H. Dugan, P. Ewart, and A. F. Purdie, *ibid.* **13**, 1416 (1976); D. J. Bradley, P. Ewart, J. V. Nicholas, J. R. D. Shaw, and D. G. Thompson, Phys. Rev. Lett. **31**, 263 (1973).

[8] T. N. Chang and X. Tang, Phys. Rev. A **44**, 232 (1991).

[9] T. N. Chang, in *Many-body Theory of Atomic Structure and Photoionization*, edited by T. N. Chang (World Scientific, Singapore, 1993), p. 213.

[10] T. N. Chang and X. Tang, Phys. Rev. A **46**, R2209 (1992).

[11] M. Gisselbrecht, D. Descamps, C. Lynga, A. L'Huillier, C.-G. Wahlstrom, and M. Meyer, Phys. Rev. Lett. **82**, 4607 (1999).

[12] T. N. Chang and T. K. Fang, Phys. Rev. A **52**, 2638 (1995).

[13] D. G. Thompson, A. Hibbert, and N. Chandra, J. Phys. B **7**, 1298 (1974).

[14] C. Mendoza and C. J. Zeippen, Astron. Astrophys. **179**, 346 (1987).

[15] T. Brage, C. Froese Fischer, and G. Miecznik, J. Phys. B **25**, 5289 (1992).

[16] T. S. Yih (private communication).

[17] T. N. Chang, Phys. Rev. A **36**, 447 (1987); **41**, 4922 (1990).

[18] M. H. Sayyar, E. T. Kennedy, L. Kiernan, J-P. Mosnier, and J. T. Costello, J. Phys. B **28**, 1715 (1995).

[19] Y. L. Shao, C. Fotakis, and D. Charalambidis, Phys. Rev. A **48**, 3636 (1993).

[20] A. H. Kung, W. J. Chen, C. K. Ni, T. K. Fang, Y. S. Yih, and T. N. Chang, Bull. Am. Phys. Soc. **44**, 722 (1999).